2002

Thermal and electrical characteristics of a multilayer thermionic device

B. C. Lough
University of Wollongong

S. P. Lee
University of Wollongong

Z. Dou
University of Wollongong

R. A. Lewis
University of Wollongong, roger@uow.edu.au

C. Zhang
University of Wollongong, czhang@uow.edu.au

THERMAL AND ELECTRICAL CHARACTERISTICS OF A MULTILAYER THERMIONIC DEVICE

B. C. C. Lough*, S. P. Lee, Z. Dou, R. A. Lewis, and C. Zhang
Institute of Superconducting and Electronic Materials,
University of Wollongong, New South Wales, 2522, Australia.
*Email Address: bcl01@uow.edu.au

ABSTRACT

We report our recent experimental and numerical investigation into the thermal and electrical transport in GaAs-AlGaAs semiconductor multilayer structures. Electrical and thermal conduction measurements were performed on multilayer structures to determine the temperature gradient across the sample. AuGe was used for top contact metallisation, and an InGa eutectic for bottom substrate contact. Metallisation contacts were also grown directly onto the substrate in order to compare results with and without the device included. By using a variable load resistor connected in series with the device, we can accurately determine the current-voltage characteristics of the device. Thus the power input can be obtained. The temperature distribution on the top and bottom substrate was measured with micro thermocouples. Since the cooling device is grown on an n-type semiconductor substrate the effects of joule heating in the substrate had to be considered. Treating the substrate as bulk material and calculating joule heating showed that this effect is negligible. Comparing experimental measurements of the device and of the substrate alone support this. The experimental I-V characteristics of the device differ significantly in shape from theoretical I-V characteristics. This may be due to that fact that space-charge effects are not included in the currently accepted model (Richardson's equation). Due to the small size of the devices and therefore very large electric fields, this effect may be important. Work is currently being carried out to modify the model. The devices studied so far have been made from undoped GaAs-$Al_{0.07}Ga_{0.93}As$ heterostructures. For large cooling power it is a requirement that the conduction band of the layers be close to the Fermi level.

1 INTRODUCTION

The simplified equations used to describe the electronic transport in the thermionic devices are based upon Richardson's equation. We have shown that although not necessarily more efficient than a single-barrier device, multi-barrier devices are capable of delivering much more cooling power [1]. Referring to Fig. 1, the net electrical current leaving the i_{th} electrode of an N-barrier device under an applied bias δV is given by:

$$J = J_i = AT_{i-1}^2 \exp(\frac{-e\phi_{i-1}}{k_b T_{i-1}}) - AT_i^2 \exp(\frac{-e(\phi_{i-1} + \delta V_i)}{k_b T_i}) \quad i = 1, 2, \ldots, N-1 \tag{1}$$

where A is Richardson's constant given by:

$$A = (em^* k_B^2)/(2\pi^2\hbar^3) \simeq 120 \text{ A/cm}^2\text{K}^2. \tag{2}$$

The other variables are defined as:

ϕ_i = Height of i_{th} barrier (eV);	T_i = Temperature of i_{th} electrode (K);
δV_i = Potential drop across $i_t h$ barrier (V);	k_b = Boltzmann's constant;
e = Charge of electron;	m^* = Electron effective mass;

Eq. 1 is quite simplistic in that it assumes constant temperature and potential in each of the electrodes, which is incorrect for a real device. It also assumes that there is no space charge collection at the heterostructure interface. Fig. 1 shows the conduction band diagram for such an *ideal* device. The electrode (or bottom of the potential barrier) is the Fermi energy in the electrode material (GaAs), whilst the top of the barrier is the conduction band in the barrier material ($Al_{0.07}Ga_{0.93}As$).

0-7803-7571-8/02/$17.00 ©2002 IEEE

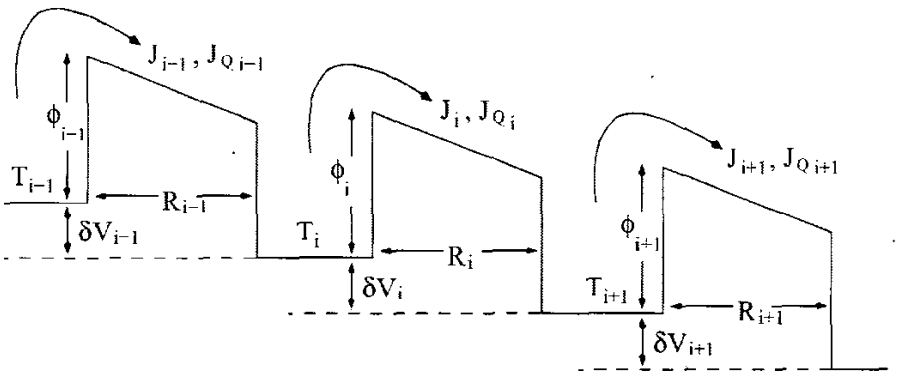

Figure 1: Energy-band diagram of 'Ideal' Multibarrier Thermionic Cooler

2 DEVICE STRUCTURE

The devices discussed in this paper were grown on a 450 μm thick GaAs wafer with an impurity concentration of $2\times\ 10^{18}$ cm^{-3}. A buffer layer of 100 nm n$^+$GaAs was grown before 10 alternating layers of undoped GaAs-$Al_{0.07}Ga_{0.93}As$ each of 50 nm. The devices were grown by the Australian National University. Because of some design flaws, no cooling has been observed in the samples. On analysis of the data, this result is in agreement with theory. The main reason for no observed cooling is because of the use of undoped material for the device. For high cooling power, it has been shown that the barrier heights at room temperature must be less than 300 meV [2]. In our samples this value is even lower, due to the thermal resistance of the materials used. Referring to Eq. 3 and Eq. 4, a low thermal resistance lowers the net energy current achievable for a device. The *conduction band offset* between materials was designed to be ~75 meV. A barrier height of 75 meV will theoretically produce measurable cooling at room temperature. Unfortunately, because of the use of undoped material, the conduction band edge of the electrodes sits at ~150 meV above the Fermi energy. This gives an effective barrier height of ~225 meV - too large to achieve any appreciable cooling at room temperature. Regardless of this, it is still beneficial to model the I-V characteristics of the device. By doing so, it is possible to see how well equation Eq. 1 does model real devices.

3 IDEAL DEVICE EQUATIONS

In addition to the electric current equation described in Eq. 1 there are two energy current equations that must be solved. Assuming net heat current flow is from left to right in Fig. 1, the energy current entering the ith electrode (from the left) is given as

$$\begin{aligned} J_{Qi}^{in} &= (\phi_{i-1}+\delta V_i+\frac{2k_bT_{i-1}}{e})AT_{i-1}^2\exp(\frac{-e\phi_{i-1}}{k_bT_{i-1}}) \\ &\quad -(\phi_{i-1}+\delta V_i+\frac{2k_bT_i}{e})AT_i^2\exp(\frac{-e(\phi_{i-1}+\delta V_i)}{k_bT_i}) \\ &\quad \frac{T_i-T_{i-1}}{R_i} \qquad i=1,2,\ldots,N-1 \end{aligned} \tag{3}$$

and the energy current leaving the ith electrode (to the right) is given as

$$\begin{aligned} J_{Qi}^{out} &= (\phi_i+\frac{2k_bT_i}{e})AT_i^2\exp(\frac{-e\phi_i}{k_bT_i}) \\ &\quad -(\phi_i+\frac{2k_bT_{i+1}}{e})AT_{i+1}^2\exp(\frac{-e(\phi_i+\delta V_{i+1})}{k_bT_{i+1}}) \\ &\quad -\frac{T_{i+1}-T_i}{R_{i+1}} \qquad i=1,2,\ldots,N-1 \end{aligned} \tag{4}$$

where R_i is the thermal resistivity of the ith barrier.
For continuity of energy current, $J_{Qi}^{in}=J_{Qi}^{out}$.
NOTE: $J_{Qi}^{in}-J_{Q(i-1)}^{out}=\delta V_iJ\neq 0$, where δV_iJ is the work needed to produce cooling across the i^{th} barrier.

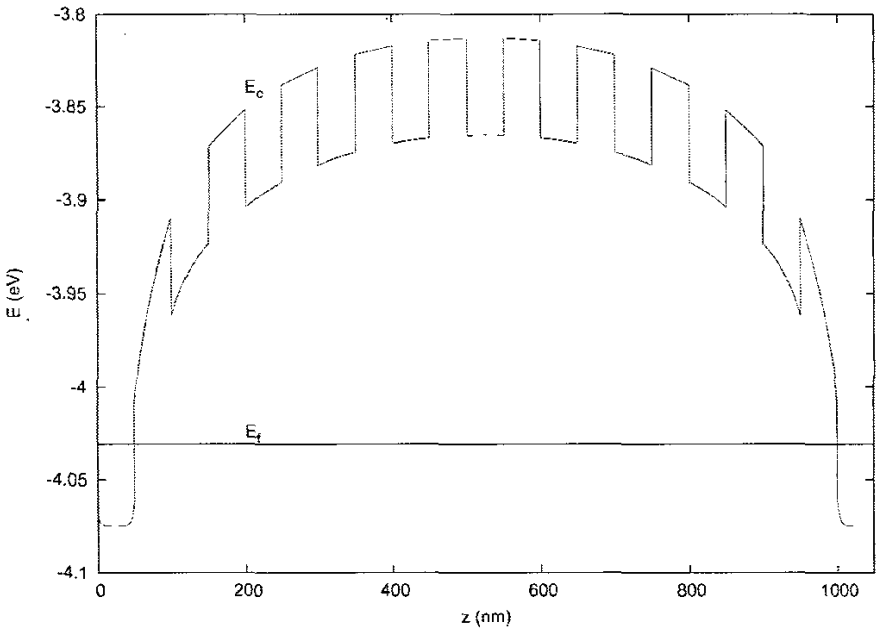

Figure 2: Energy-band diagram of multibarrier thermionic cooler calculated using Poisson's equation (400 μm substrate not included).

Equations 1, 3 and 4 are solved in order to preserve electric and energy current continuity. They are used to calculate the I-V characteristics of the device. In a recent paper we have discussed the difference between the experimental I-V characteristics and the ones given by the above equations [3]. It was noted that space charge accumulation is not accounted for in the above equations. Because of the small geometry of the device (barrier widths of $\sim$50 nm), large electric fields can be set up. As a result, the space charge potential between electrodes can become important. Under certain circumstances, this potential can be approximated very accurately by image force lowering [4]. When this approximation was used, the theoretical I-V characteristics of the devices did come closer to those obtained from experiment, but this new term does not sufficiently explain the discrepancy. In order to develop the theoretical model further, we have used first principles to first calculate the 'real' band structure of the device via *Poisson's Equation*.

4 FIRST PRINCIPLES APPROACH

Fig. 2 shows the energy band diagram for the first-generation devices calculated using Poission's Equation:

$$\nabla \cdot [\epsilon_s(z)\nabla\phi(z)] = \rho(z) \tag{5}$$

where the position-dependent variables are defined as:

$\epsilon_s(z)$ = Permittivity of material; $\phi(z)$ = Electrostatic potential; $\rho(z)$ = Charge concentration;

The equation was solved numerically using an array of points spaced sufficiently to allow convergence. Because of the geometry of the device, the equation only needs to be solved in 1-D. It is immediately obvious that this method will represent the device better than the idealised equations of the previous section. Fig. 2 shows that band-bending due to charge accumulation is a very important factor that must be taken into consideration. Solving the electrical transport equations via this method is advantageous in that space-charge effects do not need to be included explicitly in the equations. They are an inherent part of the system as long as Eq. 5 is satisfied. The band diagram in Fig. 2 shows that the conduction band in the barrier material is around 225 meV above the Fermi energy in the electrode material, giving an effective barrier height of the same size.

5 RESULTS AND ANALYSIS

The theoretical I-V characteristics of the devices were calculated using the freeware computer program *SimWindows32*. This program calculates properties of semiconductor devices via an input file giving the device structure. Fig. 3 shows both the theoretical and experimental I-V characteristics of one of the devices. The results shown

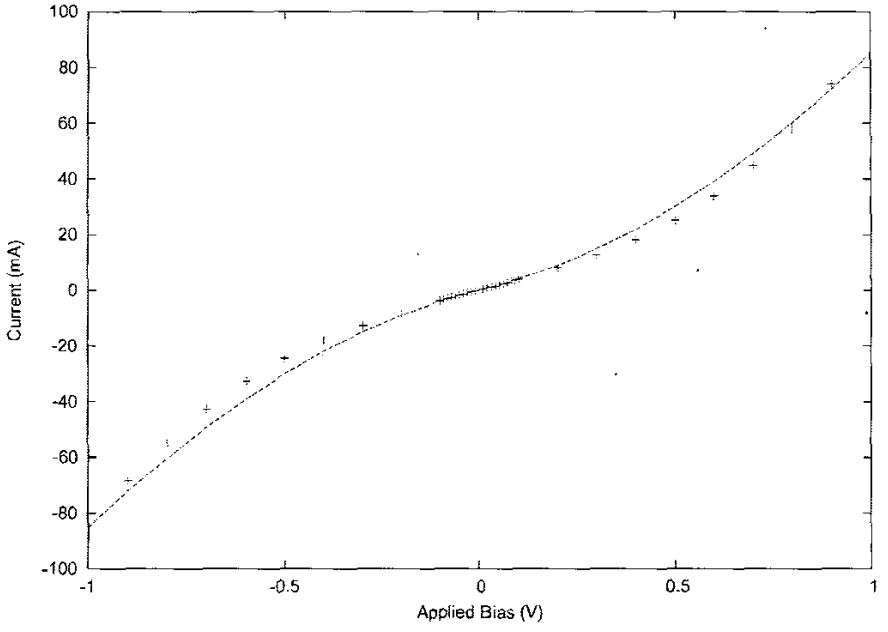

Figure 3: Experimental (+) and Theoretical (-) I-V characteristics

are for a device with a 3 mm radius. As can be seen from the figure, there is very close agreement with the experimental results. There are two major factors which explain why no cooling was observed in the devices. The first, as already discussed, is that the effective barrier height of the structure is close to 225 meV. For the material that we used to produce the samples (GaAs), this barrier height needs to be significantly lower in order for there to be sufficient power to achieve cooling at room temperature. The second factor, perhaps more important than the first, has to do with the actual structure of the device. For efficient cooling via thermionic transport, electrons must be able to travel ballistically across the potential barrier. For this to occur, the barrier width must be less than the mean free path for electrons. Typically, this value is ~50-100 nm [5]. Referring to Fig. 2, from the point of view of electrons at the Fermi energy, the device structure can be approximated by a single potential barrier of height 225 meV. This means that the transport will not be ballistic and there may be considerable scattering. Once again, this is may be overcome by using doped material.

6 CONCLUSION

Because of some fundamental design flaws in these devices - namely, the use of undoped material - no cooling was observed. New devices have been made to remedy this, and device characterisation is currently being carried out. The results show that space-charge effects are very important in these devices (because of the high electric fields due to small device geometry) and should be included in any analysis of the devices. By using numerical techniques to solve Poisson's Equation and to calculate current under non-equilibrium conditions, these effects are included and give good agreement with experimental data.

Acknowledgement: This work is supported in part by the Australian Research Council and Email Ltd.

REFERENCES

[1] B. C. Lough, S. P. Lee, Z. Dou, R. A. Lewis, C. Zhang, *Multilayer thermionic cooling in semiconductor heterostructures*, Australian Institute of Physics 15th Biennial Congress 2002 Proceedings. In Print.

[2] G. D. Mahan, *Thermionic Refrigeration*, J. Appl. Phys. **76**, 7 (1994).

[3] B. C. Lough, S. P. Lee, Z. Dou, R. A. Lewis, C. Zhang, *Investigation into space charge effects in I-V characteristics of multi-layer semiconductor thermionic devices*, International Conference on Superlattices, Nano-Structures and Nano-Devices 2002 Conference Proceedings. In Print.

[4] J. B. Scott, *Extension of Langmuir space-charge theory into the accelerating field range*, J. Appl. Phys. **52**, 7 (1981).

[5] G. D. Mahan, J. O. Sofo, M. Bartkowiak, *Multilayer thermionic refrigerator and generator*, J. Appl. Phys. **83**, 9 (1998).